# Conversion of Intensity-Averaged Photon Correlation Spectroscopy Measurements to Number-Averaged Particle Size Distributions. 1. Theoretical Development

Leo H. Hanus and Harry J. Ploehn*

*Department of Chemical Engineering, University of South Carolina, Swearingen Engineering Center, Columbia, South Carolina 29208*

*Received July 30, 1998. In Final Form: February 8, 1999*

Formulas for converting the intensity-averaged particle diameter and polydispersity obtained from quadratic cumulants (QC) analysis of photon correlation spectroscopy (PCS) data to the number-weighted mean and variance of assumed particle size distribution (PSD) forms are derived. The approach of Thomas[16] for log−normal PSDs is used to derive expressions for normal and Schultz−Zimm particle size distributions (PSDs) assuming Rayleigh scattering. Additionally, expressions for the opposite conversion (from the mean and variance of a number-weighted PSD to an intensity-averaged diameter and polydispersity) are derived for normal PSDs using the Guinier approximation of the Rayleigh−Debye−Gans (RDG) form factor for spheres. Heuristics are developed for correcting the PCS-QC-measured polydispersity $Q$ (known to be strongly affected by experimental and data analysis error) to facilitate the application of the conversion formulas. The conversion formulas and corrective heuristics are then used to re-examine previously published comparisons of PCS and transmission electron microscopy (TEM) average particle size measurements. Additionally, the PSDs generated from PCS-QC results using the conversion formulas are compared with the TEM-measured PSD for a Stöber silica suspension. These comparisons show that, despite the assumption of Rayleigh scattering, the intensity to number-weighting conversion formulas applied using the $Q$ corrective heuristics produce reasonably accurate results outside the limits of Rayleigh scattering theory.

## Introduction

Photon correlation spectroscopy (PCS)[1−7] is a quasi-elastic dynamic light-scattering technique commonly used to characterize nanometer to submicron-sized colloidal particles. Laser illumination of colloidal particles undergoing Brownian motion produces a randomly fluctuating scattered intensity signal with a temporal behavior dependent on the particles' size and shape. The time dependence of the fluctuations can be determined by autocorrelating the scattered intensity signal. For spherical particles, the scattered intensity autocorrelation function (ACF) decays exponentially with a decay constant $\overline{\Gamma}$ proportional to the intensity-weighted average Brownian diffusion coefficient $\overline{D_0}$. In the limit of low particle concentration, hydrodynamic interactions can be neglected, and the intensity-weighted average particle diameter $\overline{d_{\mathrm{PCS}}}$ can be calculated using the Stokes−Einstein equation

$$\overline{d_{\mathrm{PCS}}} = \frac{k_{\mathrm{B}}T}{3\pi\eta\overline{D_0}} \tag{1}$$

where $k_{\mathrm{B}}$ is the Boltzmann constant and $\eta$ and $T$ are the solvent viscosity and temperature.

A variety of PCS data analysis techniques[3,8] can accurately extract $\overline{d_{\mathrm{PCS}}}$ from measured ACF data. Predicting particle size distributions (PSDs) is more problematic. The most rigorous analysis approach involves a numerical Laplace inversion, which is mathematically ill-conditioned. To overcome this problem, various data analysis methods have been developed, including non-negative least squares, CONTIN, and maximum entropy analysis.[3,8] However, noise in the scattered intensity signal and the dependence of the scattered intensity on the square of the particle volume make resolution of broad or multimodal PSDs difficult regardless of the data analysis method used. Because of these limitations, simple analysis methods (such as single-exponential fitting or the method of cumulants[9−11]) often estimate $\overline{d_{\mathrm{PCS}}}$ as well as the more complex inversion methods.

The accuracy of the average particle diameter obtained from PCS measurements is commonly evaluated via comparison with transmission electron microscopy (TEM) measurements. For routine measurements, PCS analysis is desirable because it is faster and more convenient than TEM image analysis and does not require removal of the suspending solvent. However, TEM analysis yields a number-weighted particle size distribution (PSD) from which the more representative number-weighted average particle diameter[12,13] ($\overline{d_{\mathrm{TEM}}}$) can easily be calculated. The

* To whom correspondence should be addressed. Phone: (803) 777-7307. Fax: (803) 777-8265. E-mail: ploehn@engr.sc.edu.

(1) PCS is also commonly referred to as dynamic light scattering (DLS) and quasi-elastic light scattering (QELS) and less commonly as intensity fluctuation spectroscopy (IFS).

(2) Schätzel, K. *Adv. Colloid Interface Sci.* **1993**, *46*, 309−332.
(3) Finsy, R. *Adv. Colloid Interface Sci.* **1994**, *52*, 79−143.
(4) Barth, H. G.; Flippen, R. B. *Anal. Chem.* **1995**, *67* (12), 257R−272R.
(5) Provder, T. *Prog. Org. Coat.* **1997**, *32*, 143−153.
(6) *Appl. Opt.* **1997**, *36* (30), 7477−7677.
(7) Haskell, R. J. *J. Pharm. Sci.* **1998**, *87* (2), 125−129.
(8) Stepanek, P. In *Dynamic Light Scattering: The Method and Some Applications*; Brown, W., Ed.; Clarendon Press: Oxford, 1993.
(9) Koppel, D. E. *J. Chem. Phys.* **1972**, *57* (11), 4814−4820.
(10) Shaumeyer, J. N.; Briggs, M. E.; Gammon, R. W. *Appl. Opt.* **1993**, *32* (21), 3871−3878.
(11) Beretta, S.; Lunelli, L.; Chirico, G.; Baldini, G. *Appl. Opt.* **1996**, *35* (19), 3763−3770.
(12) Weiner, B. B.; Tscharnuter, W. W. In *Particle Size Distribution: Assessment and Characterization*; Provder, T., Ed.; ACS Symposium Series 332; American Chemical Society: Washington, DC, 1987.
(13) Finsy, R.; Jaeger, N. D. *Part. Part. Syst. Charact.* **1991**, *8*, 187−193.

10.1021/la980958w CCC: $18.00 
Published on Web 04/02/1999

difference between the intensity-weighted PCS and number-weighted TEM averages can be considerable. A large part of the difference is due to the type of average (intensity-weighted versus number-weighted) and is therefore a function of the particle polydispersity. However, other contributions to the difference can come from the basis of the experimental approaches and from approximations in the data analysis methods. For example, TEM image analysis is based on a somewhat subjective sampling of a relatively small number (generally less than a thousand) of single particles. Conversely, the dilute suspension volume probed by PCS typically contains on the order of a million particles and may contain particle aggregates and dust. Additionally, experimental effects such as particle shrinkage under the electron beam[14,15] for TEM or noise in the intensity ACF for PCS can impact the analysis results. Consequently, it is difficult to assess the relative importance of these contributions to the difference between PCS and TEM measurements, and this complicates the evaluation of the accuracy of the analysis methods.

Approximate methods for converting the results of simple PCS analysis techniques to number-weighted PSDs have been developed for two reasons: first, to put the PCS-based and TEM-based measures of average particle diameter on a common basis for comparison, and second, to generate PSD predictions from PCS measurements. The methods begin by assuming a functional form of the PSD. For example, formulas for converting the intensity-averaged particle diameter and polydispersity obtained from quadratic cumulants (QC) analysis of PCS data to log−normal PSDs have been developed,[16,17] and indirect methods are available for conversion to rectangular,[18] normal,[18,19] and Schultz−Zimm[20,21] PSDs. In this paper, the conversion approach developed by Thomas[16,22] for log−normal PSDs will be used to derive general expressions for converting QC analysis results to normal and Schultz−Zimm PSDs. The simplicity of this approach makes it easy to understand and therefore to apply (or to extend, for example, to other PSD forms). This being said, a more extensive consideration of the approach can be found in the work and references of Thomas[16] and in works of the vintage of Brehm et al.[23] Additionally, the intensity to number-weighting conversion equations derived in this paper can also be derived from the equations presented in ref 18 for normal distributions and in ref 21 for Schultz−Zimm distributions.

The novelty of the work in this paper is not the origin or derivation of the intensity to number-weighting conversion equations presented but rather their application for converting photon correlation spectroscopy (PCS) results to a number-weighted basis in the manner presented. On the basis solely of the work of Thomas[16] (and the earlier works of that vintage), one could rightly infer that the conversion formulas developed and applied previously produce results that are so unreasonable (because of the difficulty of measuring particle polydispersity $Q$) as to make useful application impossible. Until improved measures of particle polydispersity are possible, the $Q$ correction heuristics first suggested by Thomas[16] and further developed in this paper are necessary for useful application of the conversion formulas.

From a purely theoretical viewpoint, the use of these corrective heuristics cannot be defended and therefore may be viewed with skepticism. However, from a practical experimental viewpoint, the end results will show that via use of the heuristics the conversion formulas provide a systematic way of converting PCS and TEM measurements to a common basis for comparison and evaluation. Two points are worth noting. First, the heuristics were developed for an independent data set[36] from the literature and were found to produce good results for our own data sets for different types of particles (one of which is presented in this paper). Second, through systematic use of the heuristics, the conversion formulas produce number-weighted results that closely match those obtained from a proprietary approach (i.e., via the NICOMP instrument, refs 37−39) that uses the same principles for data analysis.

As a final note, we are not advocating the modification of any parameters that can be measured with reasonable accuracy, such as the viscosity of the medium, in order to bias the PCS results. Rather, we are attempting to develop a systematic way of correcting the polydispersity obtained from PCS (which is prone to experimental and analysis error), so as to facilitate the comparison of two commonly used measures of particle size. Improved PCS estimates of polydispersity resulting from better experimental or data analysis methods may obviate the need for the $Q$ correction heuristics developed in this paper, allowing the conversion formulas to be applied directly.

## Theoretical Development

**Photon Correlation Spectroscopy.** Homodyne (single-beam) PCS experiments measure the intensity ACF $G^{(2)}$, which can be fit with the following functional form[8]

$$\frac{G^{(2)}(\tau)}{A} - 1 = g^{(2)}(\tau) - 1 = \beta\left[\int_0^\infty f(\Gamma)\exp(-\Gamma\tau)\,d\Gamma\right]^2 \quad (2)$$

where $A = \lim_{\tau\to\infty} G^{(2)}(\tau)$ is the baseline constant of the ACF, $g^{(2)}$ is the normalized intensity ACF, $\beta$ is a correction factor (of order one) related to the coherence area of the photodetector, and $f(\Gamma)$ is the intensity-weighted decay constant distribution. The decay constant $\Gamma$ is directly related to the particle diffusion coefficient $D_0$ by

$$\Gamma = q^2 D_0 \quad (3)$$

where $q = (4\pi n/\lambda)\sin(\theta/2)$ is the scattering vector, $n$ is the solvent refractive index, $\theta$ is the scattering angle, and $\lambda$ is the laser wavelength in vacuum. The baseline constant $A$ can be determined from measured values of $G^{(2)}$ at long delay times $\tau$ or can be treated as an additional fitting parameter. However, the nonlinearity of the latter regression makes this analysis rather complicated except for the simplified cases of single- or double-exponential fits.

(14) van Blaaderen, A.; Vrij, A. In *The Colloid Chemistry of Silica*; Bergna, H. E., Ed.; ACS Symposium Series 234; American Chemical Society: Washington, DC, 1994.

(15) Ketelson, H. A.; Pelton, R.; Brook, M. A. *Langmuir* **1996**, *12* (5), 1134−1140.

(16) Thomas, J. C. *J. Colloid Interface Sci.* **1987**, *117* (1), 187−192.

(17) Bogaert, H.; Douglas, P.; van der Meeren, P. *J. Chem. Soc., Faraday Trans.* **1992**, *88* (23), 3467−3474.

(18) Bargeron, C. B. *J. Chem. Phys.* **1974**, *61* (5), 2134−2138.

(19) Solution of the equations for $K_{G1}$ and $K_{G2}$ in eq 10 of ref 18 for $a_0 = \mu$ and $\sigma_a = \sigma$, where $d_{PCS} = C/K_{G1}$ and $Q = K_{G2}/K_{G1}^2$, yields identical results to those obtained in this paper for normal distributions.

(20) Horne, D. S. *J. Colloid Interface Sci.* **1984**, *98* (2), 537−548.

(21) Taylor, T. W.; Scrivner, S. M.; Sorensen, C. M.; Merklin, J. F. *Appl. Opt.* **1985**, *24* (22), 3713−3717.

(22) For clarity, eqs 16 and 17 of ref contain typographical errors and should read $\overline{d^n}/\overline{d}^n = (1+\sigma^2)^{n(n-1)/2}$ and $\overline{d^n_{1/z}} = \overline{d}^n(1+\sigma^2)^{n(n-1)/2}$, respectively. Furthermore, ref 16's $\sigma^2$ is actually $\sigma^2/\overline{d}^2$, since $\sigma^2 = [N\sum d_j^2 - (\sum d_j)^2]/[N(N-1)]$ simplifies to $\overline{d^2} - \overline{d}^2$ for $N \gg 1$.

(23) Brehm, G. A.; Bloomfield, V. A. *Macromolecules* **1975**, *8* (5), 663.

Alternatively, $G^{(2)}$ data can be converted to electric field ACF data $g^{(1)}$ prior to analysis using

$$\sqrt{\frac{G^{(2)}(\tau,\theta)}{A} - 1} = \sqrt{g^{(2)}(\tau,\theta) - 1} = \sqrt{\beta}g^{(1)}(\tau,\theta) \quad (4)$$

Difficulties in measuring the baseline $A$ complicate this conversion. At large values of $\tau$, noise sometimes produces values of $G^{(2)}$ that are less than $A$, thus creating negative numbers under the square root in eq 4. Removal of these data points or setting $\sqrt{\beta}g^{(1)} = 0$ or $-\sqrt{1-g^{(2)}}$ when $g^{(2)} < 1$ remedies the problem but can bias the regression.[3] We use Brookhaven's approach[26] and truncate the ACF data set at the delay time of the first negative data point $\tau_-$, thereby removing all of the data for $\tau \geq \tau_-$. However, it is not clear that this approach produces any less bias than the methods mentioned above.

**Method of Cumulants.** The method of cumulants[9] is a PCS data analysis technique that circumvents the direct inversion of eq 2. The method expands the natural log of $g^{(1)}$ (eq 4) in a power series in delay time

$$\ln[\sqrt{\beta}g^{(1)}(\tau,\theta)] = K_0 - K_1\tau + \frac{K_2\tau^2}{2!} - \frac{K_3\tau^3}{3!} + \frac{K_4\tau^4}{4!} - \ldots + \frac{K_n(-\tau)^n}{n!} \quad (5)$$

known as the cumulant expansion. The constants $K_j$ ($j$ = 1, 2, ..., $n$) represent the $j$th order cumulants which are related to the $j$th moments of $f(\Gamma)$.[9] The constant $K_0$ is related to $\sqrt{\beta}$. Standard least squares fitting procedures for polynomials[24] can be used to regress $K_j$ from measured $G^{(2)}$ data according to eqs 4 and 5.

As described in ref 24, a polynomial regression can account for the statistical significance of the data by weighting the data points with their respective measurement variance $w_j = \sigma_j^{-2}$, where $w_j$ is the weighting factor and $\sigma_j$ is the standard deviation of $g^{(1)}$ at the $j$th delay time $\tau_j$. Various methods[18,25] have been used to estimate the variance in $\ln[\sqrt{\beta}g^{(1)}(\tau)]$ in order to choose weighting factors for the method of cumulants regressions. The software accompanying our Brookhaven light-scattering instrument[26] uses $w_j = [g^{(2)}(\tau_j) - 1]^2 = \beta^2[g^{(1)}(\tau_j)]^4$, which, in the context of the method of cumulants, is equivalent to other weighting methods found in the literature.[10,25]

Calculation of $g^{(1)}$, selection of the regression weighting factors $w_j$, and truncation of the infinite series cumulant expansion complicate the application of eq 5 for PCS data analysis. These problems make it difficult to accurately determine cumulants with orders higher than 2. In fact, previous studies have shown[27] that including additional terms in the cumulant expansion can increase the errors in $K_1$ and $K_2$. For this reason, most PCS applications of the method of cumulants truncate eq 5 after three terms, producing a quadratic cumulant (QC) expression ($K_0 - K_1\tau + K_2\tau^2/2$).

For particles with narrow PSDs, the left-hand side of eq 5, $\ln[\sqrt{\beta}g^{(1)}(\tau)]$, is a linear function of $\tau$. Linear regression produces the slope $K_1 = -\bar{\Gamma} = -q^2\overline{D_0}$, and substitution of $\overline{D_0}$ into eq 1 leads to $\overline{d_{PCS}}$. As the polydispersity of the particles increases, a plot of ln $[\sqrt{\beta}g^{(1)}(\tau)]$ displays increasing curvature and nonzero values of $K_2$ are obtained. Values of $K_2$, when suitably normalized with $K_1^2$ to give the suspension quality factor or polydispersity index

$$Q = \frac{K_2}{K_1^2} = \frac{\overline{\Gamma^2} - \bar{\Gamma}^2}{\bar{\Gamma}^2} \quad (6)$$

provide a quantitative indication of the PSD width.

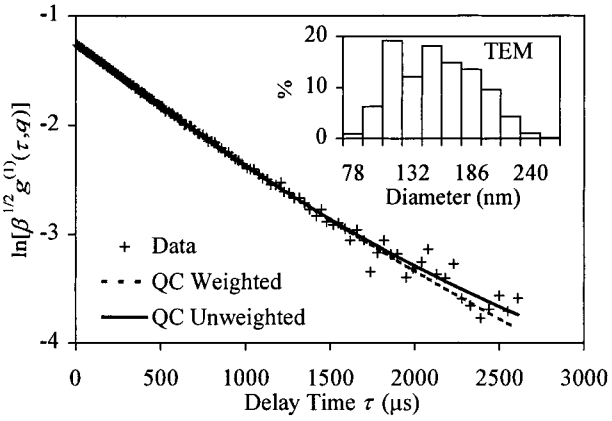


**Figure 1.** Weighted and unweighted quadratic cumulants fits of ACF data collected at $\theta = 90°$ for the Stöber[14] silica particles discussed in this paper (inset shows the number-weighted TEM histogram of particle sizes[29]).

Figure 1 shows an example of weighted and unweighted ($w_j = 1$) QC regressions of PCS data for a Stöber[14,28] silica suspension. $\overline{d_{PCS}}$ and $Q$ values of 193.2 nm and 9.6% and 181.2 nm and 14.3% were obtained from the weighted and unweighted QC fits, respectively. From a data analysis perspective, the weighted regression results are more accurate and therefore are used in the discussion that follows. TEM analysis[29] of the particles (shown in the inset of Figure 1) yielded a number-averaged diameter $\overline{d_{TEM}} = 144.8 \pm 35.9$ nm. As Figure 1 shows, the QC expansion fits the measured PCS data remarkably well despite the width of the PSD (25% of the average diameter as measured by TEM). Because the TEM PSD appears to be nearly normal (i.e., Gaussian), the distribution has little skewness or kurtosis (represented by $K_3$ and $K_4$ in eq 5), so the higher-order cumulants are small and the QC expression provides a good fit.

Despite the apparent quality of the PCS data in Figure 1, neither the average QC diameter ($\overline{d_{PCS}} = 193.2$ nm) nor the polydispersity index ($Q = 9.6\%$) compares well with the TEM results. In an attempt to improve the agreement, we averaged the results from QC fits of six independent data sets (including the one shown in Figure 1). This produced $\overline{d_{PCS}}$ and $Q$ values of 195.8 nm and 11.1%. Although this level of polydispersity compares more

(24) Press, W. H.; Flannery, B. P.; Teukolsky, S. A.; Vetterling, W. T. *Numerical Recipes*; Cambridge University Press: New York, 1988.
(25) Pusey, P. N.; Koppel, D. E.; Schaefer, D. W.; Camerini-Otero, R. D.; Koenig, S. H. *Biochemistry* **1974**, *13* (5), 952−960.
(26) Brookhaven Instruments Corporation's Data Analysis Software (BI-ISDA), version 6.5; Brookhaven Instruments Corporation (www-.bic.com): Holtsville, New York, 1989.
(27) Brown, J. C.; Pusey, P. N.; Dietz, R. *J. Chem. Phys.* **1975**, *62* (3), 1136−1144.
(28) Stöber, W.; Fink, A. E.; Bohn, E. *J. Colloid Interface Sci.* **1968**, *26* (1), 62−69.
(29) A Hitachi model H-8000 electron microscope, an AMT 1024 × 1024 digital Kodak camera system with version 1.55 software, and NIH's Image analysis software were used for the TEM analysis. The TEM images were calibrated at each magnification using a 0.5 $\mu$m diffraction grating coated with 261 nm polystyrene particles (Electron Microscopy Sciences, #80055). The particles were used as the primary size standard, and the lines of the grating, as a secondary standard. TEM analysis of 336 particles yielded a number-weighted diameter of 144.8 ± 35.9 based on ellipsoid axes measurements. Area measurements based on a circular cross section yielded equivalent results.

favorably with that from TEM, we find that $Q$ can show considerable variability from one experiment to another. Furthermore, averaging over several experiments does not improve the agreement between $\overline{d_{PCS}}$ and $\overline{d_{TEM}}$. The expressions developed in the next section provide a way of determining how much of this discrepancy is due to the difference between intensity- and number-weighted averaging.

**Number-Weighted PSDs from PCS Data: Rayleigh Scatterers.** Thomas[16] outlines a procedure for generating a number-weighted distribution $f_\#$ from the values of $\overline{\Gamma}$ and $Q$ obtained from QC analysis of PCS data (or other data analysis methods). The functional form of the distribution $f_\#$ must be specified. The intensity-weighted mean decay constant is defined as

$$\overline{\Gamma} = \frac{\sum f_{\#j} M_j^2 P_j(\Gamma_j,\theta)\Gamma_j}{\sum f_{\#j} M_j^2 P_j(\Gamma_j,\theta)} \tag{7}$$

where $f_{\#j}$, $M_j$, and $P_j$ are the number-weighted fraction, mass, and form factor[30−32] for particles with decay constant $\Gamma_j \propto 1/d_j$. In the limit of small particles or small scattering angle $\theta$ (i.e., the Rayleigh approximation[30−32]), $P(\Gamma_j,\theta) \approx 1$, and eq 7 reduces to

$$\overline{\Gamma} \approx \frac{\sum f_{\#j} M_j^2 \Gamma_j}{\sum f_{\#j} M_j^2} = \overline{\Gamma_z} \tag{8}$$

which defines a $z$-average.[13]

For spherical particles with equal densities $\rho$, the square of the particle mass varies with the sixth power of particle diameter:

$$M_j^2 = \rho^2 V_j^2 = \left(\frac{\rho\pi}{6}\right)^2 d_j^6 = C_1 d_j^6 \tag{9}$$

This result and eqs 1 and 3, written as

$$\Gamma_j = \frac{q^2 k_B T}{3\pi\eta d_j} = \left[\frac{4\pi n}{\lambda}\sin\left(\frac{\theta}{2}\right)\right]^2 \frac{k_B T}{3\pi\eta d_j} = \frac{C_2}{d_j} \tag{10}$$

can be used to simplify eq 8, giving

$$\overline{\Gamma_z} = \frac{C_1 C_2 \sum f_{\#j} d_j^6/d_j}{C_1 \sum f_{\#j} d_j^6} = \frac{C_2 \sum f_{\#j} d_j^5}{\sum f_{\#j} d_j^6} = C_2\overline{\left(\frac{1}{d}\right)_z} = \frac{C_2}{\overline{d_{1/z}}} \tag{11}$$

The last equality defines the harmonic $z$-average[13] (or $1/z$ average) diameter

$$\overline{d_{1/z}} = \frac{\sum f_{\#j} d_j^6}{\sum f_{\#j} d_j^5} = \frac{\overline{d_\#^6}}{\overline{d_\#^5}} \tag{12}$$

More generally, we can define[16] the $n$th moment of the harmonic $z$ diameter

$$\overline{d_{1/z}^n} = \frac{\sum f_{\#j} d_j^6}{\sum f_{\#j} d_j^{6-n}} = \frac{\overline{d_\#^6}}{\overline{d_\#^{6-n}}} \tag{13}$$

where $\overline{d_\#^n}$ is the $n$th moment about the origin of the number-weighted diameter distribution $f_\#$. The quantity $\overline{d_\#} \equiv \overline{d_\#^1}$ represents the number-average diameter as calculated from PCS data. Using $x$ to represent $d$ to avoid confusion in notation, the $n$th moment of $f_\#$ is defined as

$$\overline{x^n} = \int_a^\infty f_\#(x) x^n \, dx \tag{14}$$

where the lower limit $a$ depends on the range of $f_\#$ and equals $-\infty$ for the normal and Schultz−Zimm distributions and 0 for the log−normal distribution. As a check, normalized distribution functions should produce $\overline{x^0} = 1$.

The values of $\overline{d_{PCS}}$ and $Q$ obtained from QC analysis of PCS data can be expressed in terms of the moments of $f_\#$. Since $\overline{\Gamma} = C_2/\overline{d_{PCS}}$, eqs 8, 11, and 12 indicate that

$$\overline{d_{PCS}} = \frac{C_2}{\overline{\Gamma_z}} = \overline{d_{1/z}} = \frac{\overline{d_\#^6}}{\overline{d_\#^5}} \tag{15}$$

and

$$Q = \frac{\overline{\Gamma_z^2} - \overline{\Gamma_z}^2}{\overline{\Gamma_z}^2} = \frac{\overline{\Gamma_z^2}}{\overline{\Gamma_z}^2} - 1 = \frac{C_2\overline{d_{1/z}}^2}{C_2\overline{d_{1/z}^2}} - 1 = \frac{\overline{d_{1/z}}^2}{\overline{d_{1/z}^2}} - 1 = \frac{(\overline{d_\#^6}/\overline{d_\#^5})^2}{\overline{d_\#^6}/\overline{d_\#^4}} - 1 \tag{16}$$

$$= \frac{(\overline{d_\#^6})(\overline{d_\#^4})}{(\overline{d_\#^5})^2} - 1$$

assuming that the particles are Rayleigh scatterers or alternatively in the limit as $\theta$ approaches 0.[33]

Expressions for the mean $\mu$ ( $= \overline{d_\#}$) and standard deviation $\sigma$ of number-weighted distributions $f_\#$ of specified functional form can be determined by solving eqs 15 and 16 for $\mu$ and $\sigma$. This first requires evaluation of $\overline{d_\#^n}$ for $n = 4$, 5, and 6 for the specified distribution function. Table 1 gives the functional forms of the normal, log−normal, and Schultz−Zimm distributions evaluated in this paper. Figure 2 compares these distributions for one value of $\mu$ and two values of $\sigma$ to illustrate the differences between the distributions as a function of increasing distribution width.

**Rayleigh−Debye−Gans Scatterers.** According to Rayleigh−Debye−Gans (RDG) theory,[30−32] the single-particle form factor for nonadsorbing, spherical particles

(30) van de Hulst, H. C. *Light Scattering by Small Particles*; Wiley: New York, 1957.
(31) Kerker, M. *The Scattering of Light, and Other Electromagnetic Radiation*; Academic Press: New York, 1969.
(32) Bohren, C. F.; Huffman, D. R. *Adsorption and Scattering of Light by Small Particles*; Wiley: New York, 1983; pp 25−28.
(33) Pusey, P. N.; van Megen, W. *J. Chem. Phys.* **1984**, *80* (8), 3513−3520.

**Table 1. Distribution Functions Evaluated in This Paper[a]**

| distribution | $f_{\#}(x)$ |
|---|---|
| normal (Gaussian) | $\frac{\exp[-(x-\mu)^2/2\sigma^2]}{\sqrt{2\pi\sigma^2}}$ |
| log−normal[16,43] | $\frac{\exp[-\{\ln(x)-\mu_{LN}\}^2/2\sigma_{LN}^2]}{x\sqrt{2\pi\sigma_{LN}^2}}$ where $\mu_{LN}=\ln(\mu)-\sigma_{LN}^2/2$ and $\sigma_{LN}^2=\ln[1+(\sigma/\mu)^2]$ |
| Schultz−Zimm[20,21,44,45] | $\left[\frac{x(z+1)}{\mu}\right]^{z+1}\frac{\exp[-x(z+1)/\mu]}{x\Gamma(z+1)}=\left[\frac{x\mu}{\sigma^2}\right]^{\mu^2/\sigma^2}\frac{\exp[-x\mu/\sigma^2]}{x\Gamma(\mu^2/\sigma^2)}$ where $z=\mu^2/\sigma^2-1$ |

[a] $x \equiv d_{\#}$, $\mu=\overline{d_{\#}}$, $\sigma^2=\overline{d_{\#}^2}-\overline{d_{\#}}^2=\int(x-\mu)^2 f(x)\,dx$ = variance of the number distribution, and $\Gamma$ = the gamma function[24].

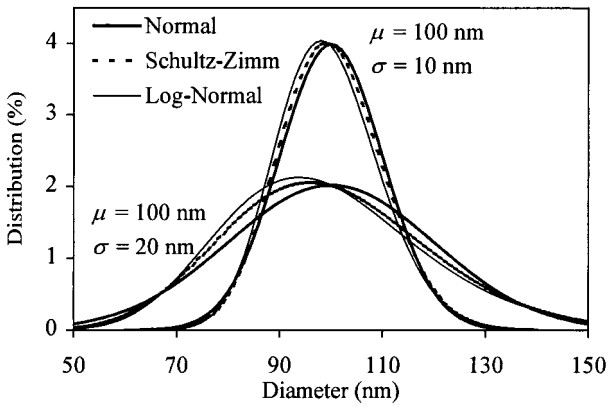


**Figure 2.** Comparison of the normal, log−normal, and Schultz−Zimm distributions.

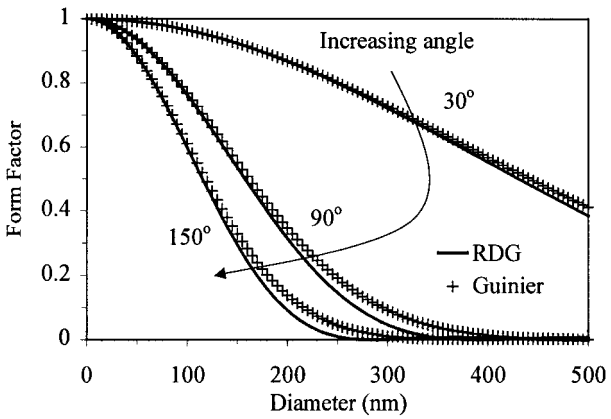


**Figure 3.** Comparison of the RDG form factor and the Guinier approximation $\exp(-0.05q^2d_{\#}^2)$ as a function of particle size in water at 20 °C for three different scattering angles (30, 90, and 150°).

of radius $R$ is

$$P(q,R)=\frac{9\pi J_{3/2}^2(qR)}{2(qR)^3}=9\left[\frac{\sin(qR)-qR\cos(qR)}{(qR)^3}\right]^2 \quad (17)$$

RDG theory requires

$$\left|\frac{n_{part}}{n}-1\right| \ll 1 \text{ and } \frac{2\pi n d_{\#}}{\lambda}\left|\frac{n_{part}}{n}-1\right| \ll 1$$

so that the incident light has uniform magnitude and phase within each particle.[32] If these conditions are not met, then the form factor must be calculated using a more complicated scattering theory such as Mie theory,[32] which is general for spheres.

Taylor series expansion of the sine and cosine terms in eq 17, algebraic manipulation, and recognition of the Taylor series expansion for the exponential leads to

$$P(q,R)=\exp(-0.2q^2R^2)=\exp(-0.05q^2d_{\#}^2) \quad (18)$$

the Guinier[34] approximation of eq 17. Figure 3 compares the form factors calculated using eqs 17 and 18. Form factors from eqs 17 and 18 differ by less than 5% for particle diameters less than $x$, where $x$ = 465, 170, and 125 nm for scattering angles of 30, 90, and 150°, respectively.

If we explicitly include the form factor in the derivation leading to eqs 15 and 16, we find

$$\overline{d_{PCS}}=\frac{\overline{Pd_{\#}^6}}{\overline{Pd_{\#}^5}} \quad (19)$$

and

$$Q=\frac{\overline{(Pd_{\#}^6)}\,\overline{(Pd_{\#}^4)}}{\overline{(Pd_{\#}^5)}^2}-1 \quad (20)$$

Using eq 18 for $P$, the required moments can be evaluated to express $\overline{d_{PCS}}$ and $Q$ in terms of $\mu$ ( = $\overline{d_{\#}}$) and $\sigma$ of a normal, number-weighted PSD $f_{\#}$.

## Results and Discussion

**Rayleigh Scatterers—Average Diameters.** We used Maple V Release 4 to evaluate the fourth-, fifth-, and sixth-order moments of the distributions in Table 1 and to solve for the parameters ($\mu$ and $\sigma$) of the number-weighted distributions using eqs 15 and 16. The expressions obtained for normal, log−normal, and Schultz−Zimm distributions are summarized in Table 2. The real root of the polynomial expression derived for the normal distribution can be evaluated using the Newton−Raphson method[24] (e.g., via the RTSAFE FORTRAN subroutine in ref 24). Alternatively, the simple series approximation shown in Table 2 can be applied accurately for $Q < 0.07$.

Figure 4 shows the ratio of number-average ($\overline{d_{\#}}$) and intensity-average ($\overline{d_{PCS}}$) particle diameters as a function of $Q$ for the various distributions and the experimental ratio measured using a NICOMP PCS instrument,[37−39] which employs a proprietary conversion algorithm. For measured values of $\overline{d_{PCS}}$ and $Q$, multiplication of $\overline{d_{PCS}}$ by the corresponding correction factor from Figure 4 gives the PCS-based number-average particle diameter $\mu=\overline{d_{\#}}$ for a selected functional form of the distribution. The correction factors in Figure 5 are less than unity, indicating

(34) Guinier, A. *Ann. Phys. (Leipzig)* **1939**, *12*, 161.

**Table 2. General Expressions for Converting the Intensity-Average Particle Diameter $\overline{d_{PCS}}$ and the Polydispersity Index $Q$ to the Mean $\mu$ and Standard Deviation $\sigma$ of Various Number-Weighted Particle Size Distributions**

| distribution | formulas for number-weighted mean $\mu$ and standard deviation $\sigma$ |
|---|---|
| normal (Gaussian) | $\mu =$ real root of $\left\{\begin{matrix}25(1+Q)^3y^5 - 75(1+Q)^2y^4 + 5(19+29Q+10Q^2)y^3 - \\ 3(21+20Q)y^2 + 3(7+5Q)y - 3\end{matrix}\right\}\overline{d_{PCS}}$ |
| | $\approx [1 - 5(Q - 3Q^2 - 25Q^3 - 163Q^4 - 849Q^5) + O(Q^6)]\overline{d_{PCS}}$ for $Q < 0.07$ |
| | and $\sigma = \overline{d_{PCS}}\sqrt{\dfrac{1-\mu/\overline{d_{PCS}}}{5(1+Q)}}$ |
| log−normal | $\mu = \dfrac{\overline{d_{PCS}}}{(1+Q)^5}$ and $\sigma = \mu\sqrt{Q}$ |
| Schultz−Zimm | $\mu = \overline{d_{PCS}}\left(\dfrac{1-4Q}{1+Q}\right)$ and $\sigma = \overline{d_{PCS}}\dfrac{\sqrt{Q(1-4Q)}}{1+Q}$ |

$y = \overline{d_\#}/\overline{d_{PCS}}$

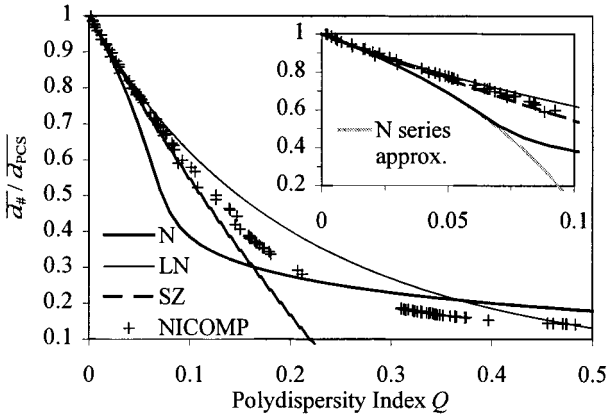


**Figure 4.** Ratio of the intensity-weighted diameter $\overline{d_{PCS}}$ to the number-weighted diameter $\overline{d_\#}$ for normal (N), log−normal (LN), and Schultz−Zimm (SZ) distributions as functions of the polydispersity index $Q$. The cross (+) data are the experimentally measured ratio obtained from the NICOMP instrument. The inset shows a magnified view for small $Q$.

that $\overline{d_\#}$ is always less than $\overline{d_{PCS}}$, at least for the three distributions considered here. For low values of $Q$, the correction factor $\overline{d_\#}/\overline{d_{PCS}}$ becomes independent of the functional form of the distribution.[35] As $Q$ increases, the assumed form of the distribution has a strong effect on $\overline{d_\#}/\overline{d_{PCS}}$: the disparity between $\overline{d_\#}$ and $\overline{d_{PCS}}$ is greater for the normal distribution than for the Schultz−Zimm or log−normal distribution. Figure 4 also shows that the correction factor for the Schultz−Zimm distribution approaches zero and is therefore invalid for $Q > 25\%$.

Thomas[16] compares values of $\overline{d_{TEM}}$ (the TEM-based number-average diameter) with values of $\overline{d_\#}$ derived from PCS data (published by Douglas et al.[36]) for several suspensions of poly(butyl-2-cyanoacrylate) and polystyrene latex particles (with unknown PSD forms). Table 3 shows the conversion of the measured values of $\overline{d_{PCS}}$ and

**Table 3. Conversion of Intensity-Weighted Average Particle Diameters from PCS (As Measured by Thomas, ref 16) to Number-Weighted Average Particle Diameters for Various Forms of the Distribution Function[a]**

| quadratic cumulants | | | TEM | log−normal | | Normal | | Schultz−Zimm | |
|---|---|---|---|---|---|---|---|---|---|
| $d_{PCS}$ | $Q_{PCS}$ (%) | $Q_{calc}$ (%) | $d_{TEM}$ | $d_\#$ | $\%\Delta^b$ | $d_\#$ | $\%\Delta^b$ | $d_\#$ | $\%\Delta^b$ (%) |
| Using $Q_{calc} = Q_{PCS}$ | | | | | | | | | |
| 469 | 3.3 | 3.3 | 450 | 399 | −11.2 | 383 | −15.0 | 395 | −12.2 |
| 180 | 3.7 | 3.7 | 166 | 150 | −9.4 | 142 | −14.4 | 148 | −10.7 |
| 417 | 4.4 | 4.4 | 390 | 336 | −13.8 | 307 | −21.2 | 329 | −15.6 |
| 203 | 7.9 | 7.9 | 165 | 139 | −16.0 | 93 | −43.6 | 129 | −22.1 |
| 160 | 10.3 | 10.3 | 122 | 98 | −19.8 | 61 | −50.4 | 85 | −30.2 |
| 159 | 15.0 | 15.0 | 130 | 79 | −39.2 | 50 | −61.7 | 55 | −57.5 |
| Using Thomas' Heuristic $Q_{calc} = Q_{PCS} - 0.03$ | | | | | | | | | |
| 469 | 3.3 | 0.3 | 450 | 463 | 2.9 | 463 | 2.9 | 463 | 2.9 |
| 180 | 3.7 | 0.7 | 166 | 174 | 5.0 | 174 | 4.8 | 174 | 4.9 |
| 417 | 4.4 | 1.4 | 390 | 389 | −0.3 | 386 | −0.9 | 388 | −0.5 |
| 203 | 7.9 | 4.9 | 165 | 160 | −3.2 | 142 | −14.1 | 155 | −5.8 |
| 160 | 10.3 | 7.3 | 122 | 112 | −7.9 | 79 | −34.9 | 105 | −13.6 |
| 159 | 15.0 | 12.0 | 130 | 90 | −30.6 | 55 | −57.4 | 74 | −43.3 |
| Using the Heuristic $Q_{calc} = Q_{PCS}/2.556$ | | | | | | | | | |
| 469 | 3.3 | 1.3 | 450 | 440 | −2.2 | 438 | −2.7 | 439 | −2.3 |
| 180 | 3.7 | 1.4 | 166 | 168 | 1.0 | 167 | 0.3 | 167 | 0.8 |
| 417 | 4.4 | 1.7 | 390 | 383 | −1.8 | 379 | −2.8 | 382 | −2.1 |
| 203 | 7.9 | 3.1 | 165 | 174 | 5.6 | 168 | 1.6 | 172 | 4.5 |
| 160 | 10.3 | 4.0 | 122 | 131 | 7.6 | 122 | 0.0 | 129 | 5.7 |
| 159 | 15.0 | 5.9 | 130 | 120 | −8.1 | 98 | −24.6 | 115 | −11.6 |
| Using the Heuristics $Q_{calc} = Q_{PCS}/2.556$, $Q_{PCS}/2.071$, and $Q_{PCS}/1.871$ for the Normal, Schultz−Zimm, and Log-Normal PSD Conversions, Respectively | | | | | | | | | |
| 469 | 3.3 | varies | 450 | 430 | −4.4 | 438 | −2.7 | 433 | −3.9 |
| 180 | 3.7 | varies | 166 | 163 | −1.6 | 167 | 0.3 | 164 | −1.0 |
| 417 | 4.4 | varies | 390 | 371 | −4.8 | 379 | −2.8 | 374 | −4.2 |
| 203 | 7.9 | varies | 165 | 165 | 0.0 | 168 | 1.6 | 166 | 0.4 |
| 160 | 10.3 | varies | 122 | 122 | 0.2 | 122 | 0.0 | 122 | 0.0 |
| 159 | 15.0 | varies | 130 | 108 | −16.8 | 98 | −24.6 | 105 | −19.0 |

[a] The data are presented in order of increasing values of the measured polydispersity index $Q$. [b] $\%\Delta = 100(\overline{d_{TEM}} - \overline{d_\#})/\overline{d_{TEM}}$.

(35) The work of Krieger, I. M. (*J. Macromol. Sci., Phys.* **1970**, *B4* (2), 437−440) helps to explain this observation. For narrow distributions ($\sigma/\mu \ll 1$), the distribution moments equal

$$\overline{d_\#^n} \approx \mu^n\left[1 + \frac{n(n-1)}{2}\left(\frac{\sigma}{\mu}\right)^2\right]$$

and eqs 15 and 16 yield

$$\overline{d_{PCS}} \approx \mu\left[1 + 5\left(\frac{\sigma}{\mu}\right)^2 - 50\left(\frac{\sigma}{\mu}\right)^4 + ...\right]$$

and

$$Q \approx \left(\frac{\sigma}{\mu}\right)^2 - 30\left(\frac{\sigma}{\mu}\right)^4 + ...$$

Thus, for $\sigma/\mu \ll 1$,

$$\frac{\mu}{\overline{d_{PCS}}} \approx 1 - 5Q$$

which explains the converging linear behavior of the different types of distributions as $Q$ decreases. This relation for $\overline{d_{PCS}}$ also follows from the expression of (1) Bargeron (ref 18) for normal distributions assuming a truncated RDG expression for spheres for $\sigma/\mu \ll 1$ (i.e., his equation 13) in the limit as $q$ approaches 0 and (2) Pusey and van Megen (ref 33) for Schultz−Zimm distributions using the full RDG expression for spheres (i.e., their equation 19) in the limit as $q$ approaches 0.

$Q_{PCS}$ (the data of Douglas et al.[36]) to $\overline{d}_{\#}$ through the use of the expressions given in Table 2. In addition, Table 3 compares values of number-average diameters from PCS ($\overline{d}_{\#}$) and TEM ($\overline{d}_{TEM}$).

The first part of Table 3 shows conversions of $\overline{d}_{PCS}$ to $\overline{d}_{\#}$ with calculations employing values of the polydispersity index $Q_{calc}$ equal to the measured values $Q_{PCS}$. The standard deviations were not computed because the corresponding TEM-based values were not available. As expected, the values of $\overline{d}_{\#}$ are less than $\overline{d}_{PCS}$ and closer to $\overline{d}_{TEM}$. However, for all values of $Q_{PCS}$, the values of $\overline{d}_{\#}$ are significantly less than $\overline{d}_{TEM}$. The remaining differences between $\overline{d}_{\#}$ and $\overline{d}_{TEM}$ could be due to experimental artifacts (e.g., particle shrinkage under the electron beam or noise in the PCS data), approximations in the data analysis method (e.g., inadequate TEM statistics or quadratic cumulants analysis), or approximations in the derivation of the conversion formula (e.g., assuming Rayleigh scattering or presuming the form of the distribution).

Here, we explore Thomas' hypothesis[16] that noise in the PCS data leads to measured values of the polydispersity index $Q_{PCS}$ that are too high. On the basis of an estimate[36] that a suspension of monodisperse particles would yield $Q_{PCS} \approx 0.03$, Thomas proposes the use of an adjusted polydispersity index $Q_{calc} = Q_{PCS} - 0.03$ in the calculations for converting $\overline{d}_{PCS}$ to $\overline{d}_{\#}$. The second part of Table 3 shows conversions using the Thomas heuristic. In general, the results show that the Thomas heuristic improves the agreement between $\overline{d}_{\#}$ and $\overline{d}_{TEM}$. As $Q_{PCS}$ increases, though, the difference between $\overline{d}_{\#}$ and $\overline{d}_{TEM}$ grows. The difference becomes large for relatively low values of $Q_{PCS}$, regardless of the assumed form of the distribution.

To generate estimates of $Q_{calc}$ that lead to better agreement between $\overline{d}_{\#}$ and $\overline{d}_{TEM}$, we propose a heuristic correction of the form $Q_{calc} = Q_{PCS}/C$. An optimal value of the constant $C$ minimizes the difference between $\overline{d}_{TEM}$ and $\overline{d}_{\#}$. For example, we obtain $Q_{calc} = Q_{PCS}/2.556$ by minimizing $|\overline{d}_{TEM} - \overline{d}_{\#}|$ for all of the suspensions in Table 3 (except $\overline{d}_{TEM} = 159$ nm), assuming a normal distribution. The third part of Table 3 shows the results found using this heuristic. For measured values of $Q_{PCS} \leq 15\%$, this heuristic leads to PCS-based estimates of $\overline{d}_{\#}$ that differ from $\overline{d}_{TEM}$ by less than 8%, regardless of the assumed form of the distribution. For the largest $Q_{PCS}$ value, 15%, the percentage difference between $\overline{d}_{\#}$ and $\overline{d}_{TEM}$ is much less than that found using Thomas' heuristic.

Similarly, the value of $C$ can be optimized separately for each assumed form of the distribution, leading to $Q_{calc} = Q_{PCS}/2.556$, $Q_{PCS}/2.071$, and $Q_{PCS}/1.871$ for the normal, Schultz–Zimm, and log–normal distributions, respectively. Figure 5 shows the effect of the different $C$ values for the different PSD forms on $\overline{d}_{\#}/\overline{d}_{PCS}$. For $QC = Q_{PCS} < 15\%$, $\overline{d}_{\#}/\overline{d}_{PCS}$ is nearly identical for all of the assumed PSD forms considered. This result logically follows from the way that the corrective factors were derived: by minimizing the difference between the converted results and TEM results for the data in Table 3 (from ref 36), all with unknown PSD forms and $Q_{PCS} < 15\%$. Thus, via use of the corrective factors, the assumed PSD form does not have a significant effect on the conversion results in this polydispersity range.

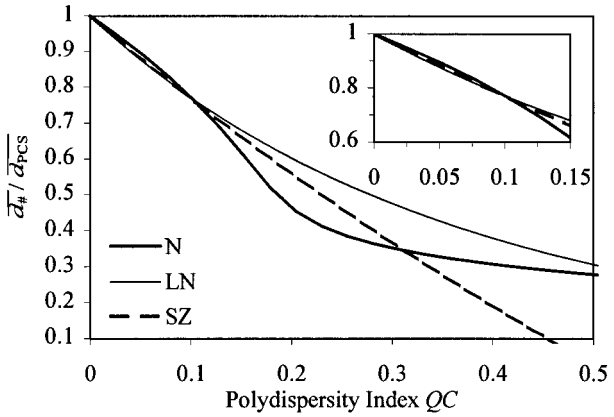


**Figure 5.** Effect of the heuristic corrective factor $C$ on the ratio of the intensity-weighted diameter $\overline{d}_{PCS}$ to the number-weighted diameter $\overline{d}_{\#}$ for normal (N), log–normal (LN), and Schultz–Zimm (SZ) distributions as functions of the polydispersity index $QC$. The inset shows a magnified view for small $QC$.

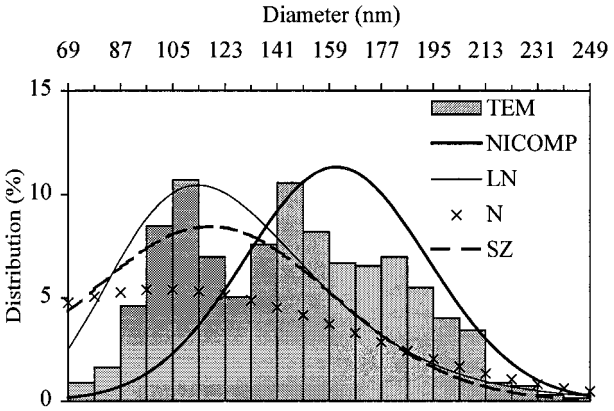


**Figure 6.** Comparison of the PSDs obtained from TEM measurements and PCS quadratic cumulants analysis converted to normal (N), log–normal (LN), and Schultz–Zimm (SZ) number-weighted distributions for the Stöber[14] silica particles discussed in this paper using the $Q$ correction heuristic $Q_{calc} = Q_{PCS} - 0.03$.

The fourth part of Table 3 employs these heuristic formulas. We see that the difference between $\overline{d}_{\#}$ and $\overline{d}_{TEM}$ decreases to less than 5% for all forms of the distribution as long as $Q_{PCS} < 15\%$. However, the more specialized heuristics lead to greater disparity between $\overline{d}_{\#}$ and $\overline{d}_{TEM}$ for the suspension with $Q_{PCS} = 15\%$. A better way of determining the heuristic corrective factors $C$ would be to minimize the difference between TEM and converted PCS results for a PSD of known distribution form using the appropriate conversion expression for that particular distribution form.

**Rayleigh Scatterers—PSDs.** In Figures 6–8, we compare TEM-measured and PCS-based PSDs for the Stöber[14] silica suspension discussed earlier (Figure 1). In these figures, the TEM-measured PSD is a number-weighted distribution based on measurements of particle diameters in TEM images.[29] The NICOMP results are number-weighted distributions obtained from that commercial PCS instrument.[37–39] The NICOMP results presented are the average of the results obtained from six different data sets. The other PSDs were generated from PCS data obtained using a Brookhaven light-scattering

(36) Douglas, S. J.; Illum, L.; Davis, S. S.; Kreuter, J. *J. Colloid Interface Sci.* **1984**, *101*, 149.

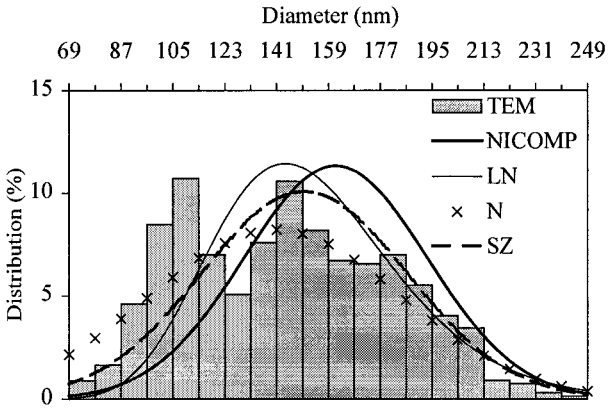


**Figure 7.** Comparison of the PSDs obtained from TEM measurements and PCS quadratic cumulants analysis converted to normal (N), log−normal (LN), and Schultz−Zimm (SZ) number-weighted distributions for the Stöber[14] silica particles discussed in this paper using the $Q$ correction heuristic $Q_{calc} = Q_{PCS}/2.556$.

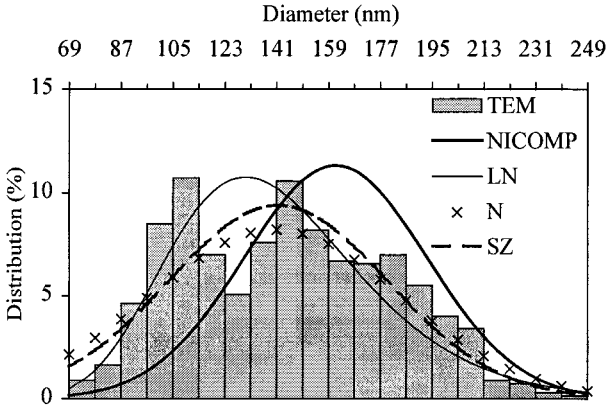


**Figure 8.** Comparison of the PSDs obtained from TEM measurements and PCS quadratic cumulants analysis converted to normal (N), log−normal (LN), and Schultz−Zimm (SZ) number-weighted distributions for the Stöber[14] silica particles discussed in this paper. The $Q$ correction heuristics $Q_{calc} = Q_{PCS}/2.556$, $Q_{PCS}/2.071$, and $Q_{PCS}/1.871$ are used for the N, SZ, and LN PSD conversions, respectively.

instrument[40] and analyzed with QC. The QC-determined values of $\overline{d_{PCS}}$ (195.8 nm) and $Q_{PCS}$ (11.1%) were converted to number-weighted normal (N), log−normal (LN), and Schultz−Zimm (SZ) distributions using the expressions given in Table 2.

The PCS-based distributions in Figure 6 employ Thomas' heuristic $Q_{calc} = Q_{PCS} - 0.03$. The NICOMP distribution ($\overline{d_{\#}} = 166.0 \pm 31.6$ nm) overestimates $\overline{d_{TEM}}$ by 14.6% and underestimates the breadth of the PSD. The N, LN, and SZ distributions better represent the actual breadth of the distribution, and they predict $\overline{d_{\#}} = 106.5 \pm 66.3$ (N), $132.6 \pm 37.8$ (LN), and $122.4 \pm 42.4$ nm (SZ), values that are 26.5%, 8.5%, and 15.4% lower than $\overline{d_{TEM}}$.

Better agreement can be achieved by using the heuristic correction formulas proposed in the previous section. We emphasize that these formulas were optimized earlier using previously published data,[36] so the predictions involve no adjustable parameters. Figure 7 uses the heuristic $Q_{calc} = Q_{PCS}/2.556$ for all assumed forms of the distribution. The estimated values of $\overline{d_{\#}}$ ($145.0 \pm 43.6$, $158.3 \pm 33.0$, and $155.1 \pm 35.5$ nm for the N, LN, and SZ distributions, respectively) differ by 0.2%, 9.3%, and 7.1% from $\overline{d_{TEM}}$. Figure 8 uses the specialized heuristics $Q_{calc} = Q_{PCS}/2.556$, $Q_{PCS}/2.071$, and $Q_{PCS}/1.871$ for the N, SZ, and LN distributions, respectively. For the LN and SZ distributions, these produce $\overline{d_{\#}}$ values of $146.8 \pm 35.8$ and $146.0 \pm 38.1$ nm, respectively, which differ from $\overline{d_{TEM}}$ by 1.4% and 0.8%. In this case, the specialized heuristics lead to better agreement between $\overline{d_{\#}}$ and $\overline{d_{TEM}}$. Although none of the assumed PSD forms can describe the exact details of the silica suspension's PSD, the averages and breadths of the PSDs are reasonably close to those of the TEM-measured PSD.

**Rayleigh−Debye−Gans Scatterers.** Assuming a normal distribution for $\overline{f_{\#}}$, substitution of eq 18 into eqs 19 and 20 and evaluation of the moments produces

$$\overline{d_{PCS}} = \frac{q^2[q^4\sigma^{10} + 30q^2\sigma^6(\mu^2+\sigma^2) + 100\mu^2\sigma^2(\mu^2+6\sigma^2) + 300\sigma^6] + 200\mu^6/3\sigma^2 + 1000(\mu^4+\sigma^4) + 3000\mu^2\sigma^2}{\mu(10+q^2\sigma^2)[q^2\sigma^4(20+q^2\sigma^2) + 20\mu^2(10+q^2\sigma^2+\mu^2/\sigma^2)/3 + 100\sigma^2]} \quad (21)$$

and

$$Q = 0.02\sigma^2\left\{\frac{q^2\sigma^4\left[\begin{array}{r}9q^6\sigma^{12}(q^2\sigma^2+50) + 300q^4\sigma^6(2\mu^4+30\sigma^4) + \\ 400q^2\sigma^2(225\sigma^6+45\mu^4\sigma^2+4\mu^6) + \\ 2000(\mu^8/\sigma^2+16\mu^6+90\mu^4\sigma^2+225\sigma^6) \\ 20000(\mu^8+30\mu^4\sigma^4+8\mu^6\sigma^2+45\sigma^8)\end{array}\right] +}{\mu^2[q^2\sigma^4(3q^2\sigma^4+60\sigma^2+20\mu^2)+10(2\mu^4+20\mu^2\sigma^2+30\sigma^4)]^2}\right\} \quad (22)$$

in terms of the mean $\mu$ and standard deviation $\sigma$ of the normal distribution. Similar expressions for the log−normal and Schultz−Zimm distributions are not presented because the required integrals $\int_a^\infty P(x)\, f_{\#}(x)x^n\, dx$ for $n = 4$, 5, and 6 could not be evaluated explicitly using Maple V. However, Pusey and van Megen[33] present a solution for Schultz−Zimm distributions with $P(x)$ defined by eq 17. Using their approach, we were able to evaluate the necessary integrals using Fourier sin and cos transforms in Maple V and to confirm the results using integral and Fourier transform tables.[41] The derived expressions agree exactly with those in ref 33 if $\Gamma(x+1)$ is used instead of $x!$.

The complexity of eqs 21 and 22 makes it difficult to solve them for $\mu$ and $\sigma$ as explicit functions of $\overline{d_{PCS}}$ and $Q$. Nevertheless, we can still use these expressions to predict values of $\overline{d_{PCS}}$ and $Q$ from the mean and variance of a TEM-measured PSD. For the TEM PSD shown in Figure

(37) Particle Sizing Systems' NICOMP model 370 with version 12.3 software; Particle Sizing Systems (www.pss.nicomp.com): Santa Barbara, CA.

(38) Nicoli, D. F.; Elings, V. B. In *NASA Laser Light Scattering Advanced Technology Development Workshop−1988*; Meyer, W. V., Ed.; NASA Conference Publication 10033; NASA: Cleveland, OH, 1989.

(39) Nicoli, D. F. In *Photon Correlation Spectroscopy: Multicomponent Systems*; Schmitz, K. S., Ed.; SPIE Proceedings Series 1430; SPIE: Bellingham, WA, 1991.

(40) Brookhaven Instruments Laser Light Scattering System consisting of BI-200SM goniometer, a BI-9000 digital correlator, version 6.5 software, and a Lexel 95A argon ion laser; Brookhaven Instruments Corporation (www.bic.com): Holtsville, NY, 1993. This instrument was operated at the laser wavelength 514 nm and the scattering angle 90°.

(41) *CRC Standard Mathematical Tables and Formulae*, 29th ed.; Beyer, W. H., Ed.; CRC Press: Boston, 1981.

(42) Wu, C. *Colloid Polym. Sci.* **1993**, *271*, 947−951.

(43) Yan, Y. D.; Clarke, J. H. R. *Adv. Colloid Interface Sci.* **1989**, *29*, 277−318.

(44) Sheu, E. Y. *Phys. Rev. A* **1992**, *45* (4), 2428−2438.

(45) The Schultz−Zimm (SZ) distributions presented in refs 21 and 43 reduce to the SZ distribution listed in Table 1 for $\sigma^2 = \sigma^2/\mu^2$.

6, substitution of $\mu = 144.8$ nm and $\sigma = 35.9$ nm into eqs 21 and 22 with $q = (4\pi n/\lambda)\sin(\theta/2) = (4\pi 1.33299/514.5)\sin(90/2) \approx 0.02302$ produces $\overline{d_{PCS}} = 171.9$ nm and $Q_{PCS} = 2.556Q_{calc} = 9.5\%$. This value of $\overline{d_{PCS}}$ is 12% lower than that actually measured by PCS (195.8 nm) for this suspension. If, instead, we substitute $\mu = 144.8$ nm and $\sigma = 35.9$ nm into eqs 15 and 16 (assuming Rayleigh scattering and a normal distribution), we find $\overline{d_{PCS}} = 181.5$ nm and $Q_{PCS} = 8.9\%$. Although this value of $\overline{d_{PCS}}$ is still 7% too low, it is a better estimate than that obtained using eqs 21 and 22, which assume RDG scattering. These observations suggest that heuristic formulas for correcting $Q$ do more than account for noise: they must also correct for inaccuracies introduced by the assumptions in the data analysis methods and conversion formulas.

Equations 19 and 20 for $\overline{d_{PCS}}$ and $Q$ plus the complete RDG form factor, eq 17, can be evaluated using numerical integration of the moments $\overline{Pd_{\#}^n}$. Using Maple V, these calculations take about 10 min to complete on a 233 MHz Intel Pentium II computer. For the silica suspension shown in Figure 6, the resulting values of $\overline{d_{PCS}}$ and $Q$ differed by less than 1% from the values obtained from eqs 21 and 22. This similarity is expected: Figure 3 indicates that eq 18 is an accurate approximation for eq 17 for $\theta = 90°$ and $\overline{d_{\#}} < 170$ nm. Similar calculations were attempted for log−normal and Schultz−Zimm distributions, but $\overline{d_{PCS}}$ and $Q$ could not be evaluated directly using Maple V. However, the results obtained numerically for normal distributions may be compared with the analytical solution for Schultz−Zimm distributions in ref 33.

**Intensity-Average Diameters from TEM Data.** In theory, we should be able to estimate the intensity-average diameter from TEM data using eq 7 (with eqs 1 and 3) without assuming any particular PSD form. Starting with the TEM PSD shown in Figure 6, use of eq 7 with form factors from Rayleigh ($P = 1$), RDG (eq 17), and Mie[32] theory produces intensity-average diameters of 180.2 ± 34.3, 183.1 ± 12.4, and 170.9 ± 16.7 nm, respectively. These values are as much as 13% lower than the value actually measured by PCS (195.8 nm).

The difference between the averages could be a result of an overestimation of the PCS diameter due to noise in the measured intensity ACF. This could explain earlier observations[36] that even suspensions with nearly monodisperse particles show significant polydispersity. To explore this hypothesis, let us again consider the silica suspension with the TEM PSD given in Figure 6. In the previous section, we found that eqs 15 and 16 (assuming a normal distribution and Rayleigh scattering) produced $\overline{d_{PCS}} = 181.5$ nm and $Q_{PCS} = 8.9\%$. If we account for the effect of noise by arbitrarily increasing the TEM standard deviation (from $\sigma = 35.9$ nm, holding $\mu = 144.8$ nm constant) until the calculated value of $Q_{PCS}$ matches the measured value of 11.1%, the calculated value of $\overline{d_{PCS}}$ becomes 195.5 nm, essentially identical to the measured value. This suggests that QC analysis of PCS data may overestimate the actual polydispersity of the PSD, perhaps due to signal noise, as suggested by Thomas.[16] Alternately, the TEM PSD may not be accurate: inclusion of a few more large particles in the PSD would increase the variance as well as $\overline{d_{TEM}}$, both leading to higher values of $\overline{d_{PCS}}$. Further comparisons of PCS and TEM data are needed to properly address this issue.

## Conclusions

The primary results of this work are the intensity to number-weighting (Table 2) and number to intensity-weighting (eqs 21 and 22) conversion formulas. The formulas in Table 2 have been presented previously in the literature (directly for log−normal[16,17] PSDs and in various forms for normal[18] and Schultz−Zimm[21] PSDs). To our knowledge, eqs 21 and 22 for normal PSDs have not been derived previously (although Pusey and van Megen[33] have derived similar expressions for Schultz−Zimm PSDs).

Analysis of earlier applications[16] of the log−normal conversion formula (Table 2) suggested that consistently reasonable agreement between $\overline{d_{\#}}$ and $\overline{d_{TEM}}$ is not possible without improved prediction of particle polydispersity by PCS. Thus, to facilitate useful application of the conversion formulas, we developed $Q$ correction heuristics (based on the suggestion of Thomas[16]) that produce better agreement between $\overline{d_{\#}}$ and $\overline{d_{TEM}}$ for wider ranges of particle polydispersity and for various assumed PSD forms. After optimizing a numerical factor in these heuristics using previously published data,[36] we find good agreement between converted PCS and measured TEM PSDs for a Stöber silica suspension. The conversion results also agree closely with the results from a NICOMP PCS instrument which employs a proprietary conversion algorithm based on the same data analysis principles. We also find that, for polydispersities less than 15%, $\overline{d_{\#}}/\overline{d_{PCS}}$ values obtained from the conversion formulas for the different assumed PSD forms essentially converge (Figure 5) when our $Q$ correction heuristics are used. This means that the assumed PSD form essentially does not matter when our $Q$ correction heuristics are used with the conversion formulas in this polydispersity range. This observation is consistent with the convergence of the PSD forms with decreasing polydispersity (Figures 2 and 4 and ref 35) and has been confirmed in the analysis of PCS and TEM data for several silica and polystyrene suspensions studied in our lab (the subject of subsequent papers).

Better estimates of $Q$ would make the use of the correction heuristics unnecessary. To this end, we have explored different experimental conditions (e.g., measurement at multiple angles and different temperatures) and alternative data analysis techniques. For example, the extrapolation techniques of Beretta et al.[11] (extrapolation to zero analysis error), Brehm and Bloomfield[23] (extrapolation to zero $q$), and Brown et al.[27] (extrapolation to zero $\overline{\Gamma}\tau_{max}$) for improved QC parameter prediction have all been explored. Additionally, the analysis approach suggested by Wu[42] was investigated. None of these methods produced improved results consistently for any of several silica and polystyrene data sets investigated. However, if improved methods of predicting PCS parameters are developed (via either experimental or data analysis enhancements), then the conversion formulas presented in this paper can be easily be applied and evaluated without the use of the $Q$ correction heuristics.

The primary limitations of the conversion formulas developed in this paper are (1) the need for correction of the PCS-measured $Q$ value and (2) knowledge of (or assumption of) a uniform PSD form for the suspension being studied. The first limitation was addressed in the previous paragraph. The second limitation means that the conversion formulas are unable to resolve complex or multimodal PSDs. However, for uniform PSDs with polydispersities less than 15%, the conversion formulas produce good results regardless of the conversion formula used (i.e., the PSD form assumed). For larger polydis-

persities, a priori knowledge of the PSD form leads to the best conversion results. However, the formulas have produced reasonable predictions (not shown in this paper) of average particle size in these cases and even for multimodal PSDs regardless of the conversion formula used. These results appear in subsequent papers (already submitted for publication) dealing with the analysis of silica and polystyrene suspensions.

The most practical benefit of the conversion formulas is that they allow us to convert PCS and TEM measures of particle size to a common averaging basis. This allows us to address the importance of the other possible contributions (already mentioned in this paper) to the difference between $\overline{d_{PCS}}$ and $\overline{d_{TEM}}$, and perhaps to answer the question of whether PCS and TEM measures of particle size can be compared at all. This being said, the implications of the light-scattering assumptions and $Q$ correction heuristics used to derive and apply the conversion formulas must be explored before firm conclusions can be drawn. This will require a critical assessment of the conversion results for suspensions of different particle types and sizes with different PSD features.

For example, the heuristic correction formulas were developed using expressions (Table 2) based on Rayleigh scattering theory. When the heuristic formulas are used with conversion expressions (eqs 21 and 22) based on RDG scattering theory, the difference between $\overline{d_{\#}}$ and $\overline{d_{TEM}}$ increases. This suggests that the heuristic corrections also account, at least in part, for inaccuracies introduced by approximations in the development of the conversion formulas and, possibly, the choice of data analysis method. The impact of PCS measurement noise on the difference between $\overline{d_{\#}}$ and $\overline{d_{TEM}}$ (the rationale behind the $Q$ correction heuristics) is another issue that needs to be investigated further. Conversion of a TEM PSD into the intensity-average diameter, either rigorously through eq 7 or assuming a PSD form through eqs 15 and 16 or the expressions in Table 2, produces similar underestimates of $\overline{d_{PCS}}$. Increasing the standard deviation in the TEM PSD to account for the effect of noise leads to better agreement between estimated and measured values of $\overline{d_{PCS}}$. We continue this critical assessment of the conversion formulas and $Q$ correction heuristics in the papers dealing with the conversion results for silica and polystyrene suspensions.

**Acknowledgment.** We acknowledge the National Science Foundation for financial support provided through Grant EHR-95-55.

LA980958W